Research Article | Vol. 8, No. 3 | 1 Mar 2018 | OPTICAL MATERIALS EXPRESS 493
Optical Materials EXPRESS

Growth, spectroscopy, and laser operation of "mixed" vanadate crystals Yb:$Lu_{1-x-y}Y_xLa_yVO_4$

Bin Zhao,[1] Yanping Ye,[1] Jianzhong Chen,[1] Haifeng Lin,[2] Ge Zhang,[2] Xavier Mateos,[3] Josep Maria Serres,[3] Magdalena Aguiló,[3] Francesc Díaz,[3] Pavel Loiko,[4] Uwe Griebner,[5] Valentin Petrov,[5] and Weidong Chen[2,5,*]

[1]*College of Chemistry, Fuzhou University, Fuzhou, 350116 Fujian, China*
[2]*Key Laboratory of Optoelectronic Materials Chemistry and Physics, Fujian Institute of Research on the Structure of Matter, Chinese Academy of Sciences, Fuzhou, 350002 Fujian, China*
[3]*Física i Cristal·lografia de Materials i Nanomaterials (FiCMA-FiCNA)-EMaS, Dept. Química Física i Inòrganica, Universitat Rovira i Virgili (URV), Campus Sescelades, E-43007 Tarragona, Spain*
[4]*ITMO University, 49 Kronverkskiy pr., 197101 St. Petersburg, Russia*
[5]*Max Born Institute for Nonlinear Optics and Short Pulse Spectroscopy, Max-Born-Str. 2a, D-12489 Berlin, Germany*
**chenweidong@fjirsm.ac.cn*

Abstract: We report on the crystal growth, structure, Raman and optical spectroscopy of novel "mixed" tetragonal vanadates, Yb:$Lu_{1-x-y}Y_xLa_yVO_4$. Optical absorption, stimulated-emission, and gain cross-section spectra of Yb^{3+} are determined for π and σ polarizations. For a Yb:$Lu_{0.74}Y_{0.23}La_{0.01}VO_4$ crystal, the absorption bandwidth is >10 nm, the σ_{SE} is 1.1×10^{-20} cm^2 at 1013 nm, the gain bandwidth is >40 nm (for π-polarization), and the radiative lifetime of the $^2F_{5/2}$ state is ~305 μs. The Stark splitting of the Yb^{3+} multiplets is determined using low-temperature (6 K) spectroscopy. A diode-pumped ***a***-cut 2 at.% Yb:$Lu_{0.74}Y_{0.23}La_{0.01}VO_4$ laser generated 5.0 W at 1044 nm with a slope efficiency of 43%. The developed materials are promising for sub-100 fs mode-locked lasers at ~1 μm.

OCIS codes: (140.3380) Laser materials; (140.3480) Lasers, diode-pumped; (140.3070) Infrared and far-infrared lasers.

References and links

1. J. Liu, V. Petrov, H. Zhang, J. Wang, and M. Jiang, "High-power laser performance of *a*-cut and *c*-cut Yb:$LuVO_4$ crystals," Opt. Lett. **31**(22), 3294–3296 (2006).
2. D. J. Jovanović, A. Chiappini, L. Zur, T. V. Gavrilović, T. N. Lam Tran, A. Chiasera, A. Lukowiak, K. Smits, M. D. Dramićanin, and M. Ferrari, "Synthesis, structure and spectroscopic properties of luminescent $GdVO_4$:Dy^{3+} and $DyVO_4$ particles," Opt. Mater. **76**, 308–316 (2018).
3. J. Liu, W. Han, H. Zhang, X. Mateos, and V. Petrov, "Comparative study of high-power continuous-wave laser performance of Yb-doped vanadate crystals," IEEE J. Quantum Electron. **45**(7), 807–815 (2009).
4. Y. Sato and T. Taira, "The studies of thermal conductivity in $GdVO_4$, YVO_4, and $Y_3Al_5O_{12}$ measured by quasi-one-dimensional flash method," Opt. Express **14**(22), 10528–10536 (2006).
5. P. A. Loiko, K. V. Yumashev, V. N. Matrosov, and N. V. Kuleshov, "Dispersion and anisotropy of thermo-optic coefficients in tetragonal $GdVO_4$ and YVO_4 laser host crystals: erratum," Appl. Opt. **54**(15), 4820–4822 (2015).
6. V. E. Kisel, A. E. Troshin, N. A. Tolstik, V. G. Shcherbitsky, N. V. Kuleshov, V. N. Matrosov, T. A. Matrosova, and M. I. Kupchenko, "Spectroscopy and continuous-wave diode-pumped laser action of Yb^{3+}:YVO_4," Opt. Lett. **29**(21), 2491–2493 (2004).
7. C. Kränkel, D. Fagundes-Peters, S. T. Fredrich, J. Johannsen, M. Mond, G. Huber, M. Bernhagen, and R. Uecker, "Continuous wave laser operation of Yb^{3+}:YVO_4," Appl. Phys. B **79**(5), 543–546 (2004).
8. J. Liu, X. Mateos, H. Zhang, J. Wang, M. Jiang, U. Griebner, and V. Petrov, "Characteristics of a continuous-wave Yb:$GdVO_4$ laser end pumped by a high-power diode," Opt. Lett. **31**(17), 2580–2582 (2006).
9. V. E. Kisel, A. E. Troshin, N. A. Tolstik, V. G. Shcherbitsky, N. V. Kuleshov, V. N. Matrosov, T. A. Matrosova, and M. I. Kupchenko, "Q-switched Yb^{3+}:YVO_4 laser with Raman self-conversion," Appl. Phys. B **80**(4), 471–473 (2005).
10. S. Rivier, X. Mateos, J. Liu, V. Petrov, U. Griebner, M. Zorn, M. Weyers, H. Zhang, J. Wang, and M. Jiang, "Passively mode-locked Yb:$LuVO_4$ oscillator," Opt. Express **14**(24), 11668–11671 (2006).

#314785 https://doi.org/10.1364/OME.8.000493
Journal © 2018 Received 1 Dec 2017; revised 31 Jan 2018; accepted 1 Feb 2018; published 5 Feb 2018

Optical Materials EXPRESS

11. J. Liu, V. Petrov, U. Griebner, F. Noack, H. Zhang, J. Wang, and M. Jiang, "Optical bistability in the operation of a continuous-wave diode-pumped Yb:$LuVO_4$ laser," Opt. Express **14**(25), 12183–12187 (2006).
12. Y. Yu, Y. Cheng, H. Zhang, J. Wang, X. Cheng, and H. Xia, "Growth and thermal properties of $YbVO_4$ single crystal," Mater. Lett. **60**(8), 1014–1018 (2006).
13. V. E. Kisel, N. A. Tolstik, A. E. Troshin, N. V. Kuleshov, V. N. Matrosov, T. A. Matrosova, M. I. Kupchenko, F. Brunner, R. Paschotta, F. Morier-Genoud, and U. Keller, "Spectroscopy and femtosecond laser performance of Yb^{3+}:$Gd_{0.64}Y_{0.36}VO_4$ crystal," Appl. Phys. B **85**(4), 581–584 (2006).
14. J. Liu, H. Zhang, X. Mateos, W. Han, V. Petrov, and J. Wang, "Low quantum defect laser oscillation of a new mixed $Yb_{0.009}$:$Y_{0.575}Gd_{0.416}VO_4$ crystal," Opt. Express **16**(22), 17729–17734 (2008).
15. A. A. Kaminskii, K. I. Ueda, H. J. Eichler, Y. Kuwano, H. Kouta, S. N. Bagaev, T. H. Chyba, J. C. Barnes, G. M. Gad, T. Murai, and J. Lu, "Tetragonal vanadates YVO_4 and $GdVO_4$ – new efficient $\chi^{(3)}$-materials for Raman lasers," Opt. Commun. **194**(1), 201–206 (2001).
16. S. A. Miller, H. H. Caspers, and H. E. Rast, "Lattice vibrations of yttrium vanadate," Phys. Rev. **168**(3), 964–969 (1968).
17. L. Z. Zhang, Z. B. Lin, and G. F. Wang, "Growth and spectral properties of Yb^{3+} doped $LaVO_4$ crystal," Mater. Res. Innov. **10**(4), 421–423 (2006).
18. S. A. Payne, L. L. Chase, L. K. Smith, W. L. Kway, and W. F. Krupke, "Infrared cross-section measurements for crystals doped with Er^{3+}, Tm^{3+}, and Ho^{3+}," IEEE J. Quantum Electron. **28**(11), 2619–2630 (1992).
19. B. Aull and H. Jenssen, "Vibronic interactions in Nd:YAG resulting in nonreciprocity of absorption and stimulated emission cross sections," IEEE J. Quantum Electron. **18**(5), 925–930 (1982).
20. P. H. Haumesser, R. Gaumé, B. Viana, E. Antic-Fidancev, and D. Vivien, "Spectroscopic and crystal-field analysis of new Yb-doped laser materials," J. Phys. Condens. Matter **13**(23), 5427–5447 (2001).
21. A. S. Yasyukevich, V. G. Shcherbitskii, V. E. Kisel', A. V. Mandrik, and N. V. Kuleshov, "Integral method of reciprocity in the spectroscopy of laser crystals with impurity centers," J. Appl. Spectrosc. **71**(2), 202–208 (2004).

1. Introduction

Tetragonal (zircon ($ZrSiO_4$) type, sp. gr. $I4_1/amd$) orthovanadate crystals, $REVO_4$ where RE = Gd, Y, or Lu, are very suitable hosts for rare-earth laser-active ions. These materials are optically uniaxial (the optical axis is parallel to the crystallographic ***c***-axis) and offer linearly polarized laser output [1-2], relatively high transition cross-sections for the dopant ions [3] and good thermo-mechanical and thermo-optical properties (high thermal conductivity, low thermal expansion, positive dn/dT coefficients and weak thermal lensing) [4-5]. Recently, $REVO_4$ crystals have been studied for Yb^{3+} doping [1,3,6–8] resulting in efficient continuous-wave (CW) [1], Q-switched [9] and sub-100 fs mode-locked (ML) oscillators [10]. Optical bistability has been also observed in CW Yb:$REVO_4$ lasers [11]. In ref [1], a diode-pumped CW ***a***-cut Yb:$LuVO_4$ laser generated 8.3 W of π-polarized output at 1031 nm with a slope efficiency of 80% (with respect to the absorbed pump power). In ref [10], a semiconductor saturable absorber mirror (SESAM) was used to generate 58-fs-long laser pulses from a ML Yb:$LuVO_4$ laser at 1036 nm at a repetition rate of 94 MHz.

In the $REVO_4$ crystals, there is a single site for accommodating the RE^{3+} ions (D_{2d} symmetry, VIII-fold O^{2-} coordination). The Yb^{3+} ions replace the RE^{3+} ones resulting in a $RE_{1-x}Yb_xVO_4$ composition. Stoichiometric tetragonal $YbVO_4$ crystals also exist but the fluorescence quenching effect is determental [12]. Besides the ordered Yb:$REVO_4$ compounds, "mixed" crystals, e.g. Yb:$Gd_{1-x}Y_xVO_4$ or Yb:$Lu_{1-x}Gd_xVO_4$, can be grown with good optical quality [3,13,14]. Due to the inhomogeneous broadening of the Yb^{3+} spectral bands as a result of the local disorder leading to slightly varying crystal field strengths, such crystals are of interest for shortening of the pulse from ML lasers. In ref [13], a SESAM ML Yb:$Gd_{0.64}Y_{0.36}VO_4$ laser generated 100-fs pulses at ~1021 nm (shorter compared to the ordered Yb:YVO_4 crystal) with a spectral bandwidth of ~33 nm (for π-polarization).

In the present work, we have grown, characterized and demonstrated CW laser operation of novel "mixed" vanadate crystals, Yb:$Lu_{1-x-y}Y_xLa_yVO_4$, featuring a strong broadening of the spectral bands due to the particular "mixture" of passive ions (Lu^{3+}, Y^{3+} and La^{3+}) with pronounced ionic radius difference.

Optical Materials EXPRESS

2. Crystal growth and structure

Crystals with two different compositions of 2.6 at.% Yb:$Lu_{0.51}Y_{0.45}La_{0.01}VO_4$ and 2 at.% Yb:$Lu_{0.74}Y_{0.23}La_{0.01}VO_4$ were grown by the Czochralski method in N_2 + 2 vol.% O_2 atmosphere using Ir crucibles and [100]-oriented undoped YVO_4 seeds. The pulling rate was 2-3 mm/h and the rotation rate was 10-30 rpm (revolutions per minute). The as-grown crystals were cooled down to room temperature (RT, 293 K) at 30–80 °C/h and annealed in air at 1200 °C for 20 h. The obtained boules with dimensions of Ø25 × 20 mm^3, Fig. 1(a),(b), were of high optical quality. The as-grown crystals had yellowish coloration which could be partially removed by annealing in air. For the spectroscopic and laser studies, 3 mm-thick rectangular samples were cut along the ***a***-axis with an aperture of 3 × 3(***c***) mm^2. They provided access to both principal light polarizations of the uniaxial vanadates, π (***E*** ∥ ***c***) and σ (***E*** ⊥ ***c***)

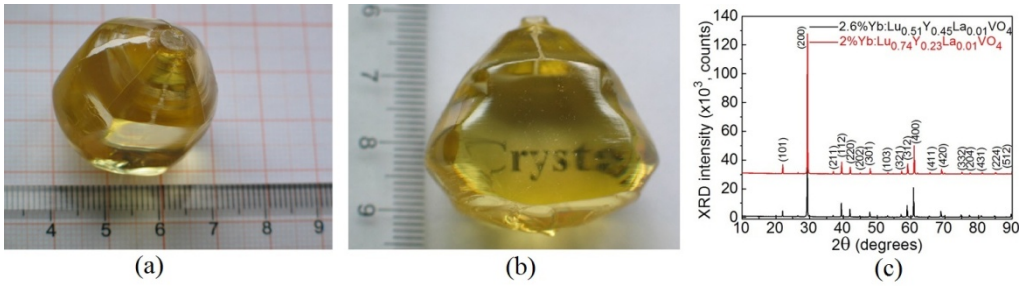

Fig. 1. (a,b) Photographs of the as-grown crystals (a) 2 at.% Yb:$Lu_{0.74}Y_{0.23}La_{0.01}VO_4$ and (b) 2.6 at.% Yb:$Lu_{0.51}Y_{0.45}La_{0.01}VO_4$ crystals; (c) X-ray powder diffraction (XRD) patterns of these crystals (the numbers denote the Miller's indices (*hkl*)).

The structure and the phase purity of the grown crystals were confirmed by X-ray powder diffraction analysis, Fig. 1(c). Both crystals are tetragonal (sp. gr. $I4_1/amd$ – D^{19}_{4h}, No. 141, formula units per unit-cell Z = 4, point group 4/*mmm*) with the following lattice parameters: $a = b = 7.076$ Å, $c = 6.266$ Å (for the Yb:$Lu_{0.51}Y_{0.45}La_{0.01}VO_4$ crystal) and $a = b = 7.056$ Å, $c = 6.253$ Å (for the Yb:$Lu_{0.74}Y_{0.23}La_{0.01}VO_4$ one). The composition of the crystals and the Yb^{3+} doping concentration were determined by Inductively Coupled Plasma (ICP) atomic spectroscopy: $N_{Yb} = 3.31 \times 10^{20}$ cm^{-3} and 2.57×10^{20} cm^{-3} for the 2.6 at.% Yb-doped and 2 at.% Yb-doped crystals, respectively.

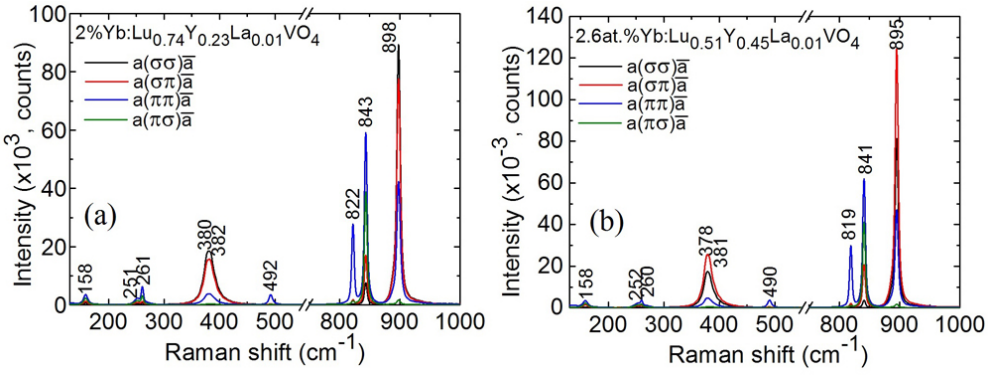

Fig. 2. Polarized Raman spectra for the ***a***-cut (a) 2 at.% Yb:$Lu_{0.74}Y_{0.23}La_{0.01}VO_4$ and (b) 2.6 at.% Yb:$Lu_{0.51}Y_{0.45}La_{0.01}VO_4$ crystals, $\lambda_{exc} = 514$ nm.

The vibrational properties of the crystals were studied by polarized Raman spectroscopy, Fig. 2. For the point group 4/*mmm*, the irreducible representations at the center of the Brillouin zone (k = 0) are: $\Gamma = (2A_{1g} + 2B_{1u}) + (B_{1g} + A_{1u}) + (A_{2g} + B_{2u}) + (4B_{2g} + 4A_{2u}) +$

Optical Materials EXPRESS

($5E_g$ + $5E_u$) of which 12 ($2A_{1g}$ + B_{1g} + $4B_{2g}$ + $5E_g$) are Raman-active [15]. For the studied crystals, a total of 9 modes are clearly resolved in the spectra and the maximum phonon frequency hvph is 898 cm^{-1} ($Yb:Lu_{0.74}Y_{0.23}La_{0.01}VO_4$) and 895 cm^{-1} ($Yb:Lu_{0.51}Y_{0.45}La_{0.01}VO_4$). These lines are assigned as $v_1(A_{1g})$ and correspond to internal symmetric vibrations of the tetrahedral $[VO_4]^{3-}$ groups [16].

3. Optical spectroscopy

The absorption cross-section spectra (σ_{abs}) for the studied crystals are shown in Fig. 3(a, c) with the polarizations along π and σ. For $Yb:Lu_{0.74}Y_{0.23}La_{0.01}VO_4$, the maximum σ_{abs} corresponds to π-polarization, 5.2×10^{-20} cm^2 at 984.5 nm (zero-phonon line, ZPL, the full width at half maximum (FWHM) of the absorption peak is 10.4 nm). For σ-polarization, the peak σ_{abs} value is 2.7 times lower and it is reached at 969.6 and 984.6 nm. For the $Yb:Lu_{0.51}Y_{0.45}La_{0.01}VO_4$ crystal, σ_{abs} for π-polarization is slightly lower, namely 4.4×10^{-20} cm^2 at 984.7 nm while the FWHM of the absorption peak is broader, 13.1 nm. Similarly, the absorption spectrum for σ-polarization features two peaks at 969.9 and 984.7 nm with 2.4 times lower σ_{abs}. The determined FWHM values for the ZPL are broader than those in $Yb:REVO_4$ (RE = Gd, Y and Lu) crystals and in the previously studied "mixed" vanadates $Yb:Gd_{1-x}Y_xVO_4$ and $Yb:Lu_{1-x}Gd_xVO_4$ [3]. The addition of large La^{3+} ions (ionic radius: 1.16 Å compared to 1.053 Å for Gd^{3+}, 1.019 Å for Y^{3+}, and 0.977 Å for Lu^{3+} in VIII-fold O^{2-} coordination) is expected to contribute to the distortion of the crystal field and the observed spectral broadening. Indeed, it is known that $LaVO_4$ is monoclinic (monazite ($(Ce,La)PO_4$) type, sp. gr. $P2_1/n$) [17].

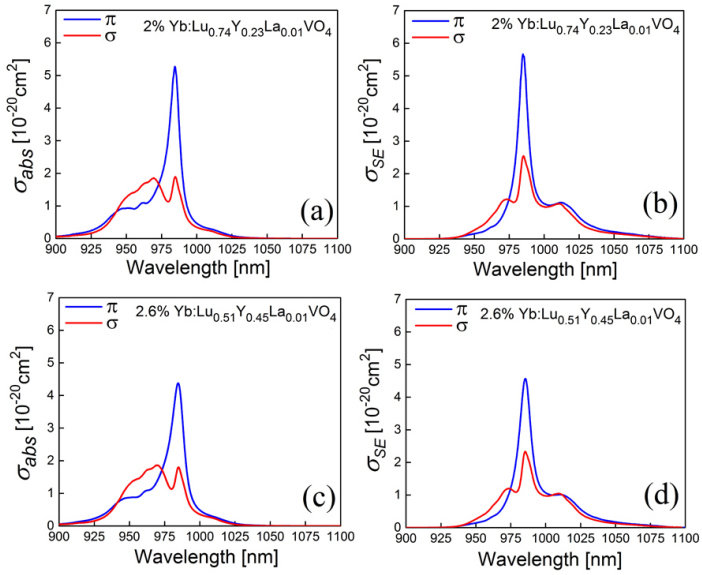

Fig. 3. Room temperature (293 K) optical spectroscopy of (a, b) 2 at.% $Yb:Lu_{0.74}Y_{0.23}La_{0.01}VO_4$ and (c,d) 2.6 at.% $Yb:Lu_{0.51}Y_{0.45}La_{0.01}VO_4$ crystals: (a,c) absorption cross-sections, σ_{abs}, and (b, d) stimulated-emission cross-sections, σ_{SE}, for π and σ light polarizations.

The stimulated-emission cross-sections, σ_{SE}, were calculated with a combination of the reciprocity method (RM) [18] and the Füchtbauer-Ladenburg (F-L) formula [19]. The latter method was applied for the long-wavelength part of the σ_{SE} spectra (>1050 nm). In the RM, the determined Yb^{3+} Stark splitting was considered (see Fig. 6). In the F-L method, the measured polarized luminescence spectra and the calculated radiative lifetimes, τ_{rad} ($^2F_{5/2}$), were used (see Fig. 3 and 4). The results obtained by the two methods were in reasonable agreement having in mind the effect of reabsorption on the measured luminescence spectra.

Optical Materials EXPRESS

The results for σ_{SE} are shown in Fig. 3(b, d). In the spectral range where laser operation is expected, σ_{SE} amounts to ~1.1 × 10^{-20} cm^2 at 1013 nm (π) or 1010 nm (σ) (for Yb:$Lu_{0.74}Y_{0.23}La_{0.01}VO_4$). For the Yb:$Lu_{0.51}Y_{0.45}La_{0.01}VO_4$ crystal, the corresponding σ_{SE} are slightly lower, 1.0 × 10^{-20} cm^2 at 1012 nm (π) or 1009 nm (σ).

The measured luminescence decay curves (excitation at 980 nm, luminescence at 1010 nm), see Fig. 4, are clearly single-exponential for both crystals and the decay time τ_{lum} is 363 μs (for the Yb:$Lu_{0.74}Y_{0.23}La_{0.01}VO_4$ crystal). For the Yb:$Lu_{0.51}Y_{0.45}La_{0.01}VO_4$ crystal, τ_{lum} is longer, 384 μs, explaining the difference in the transition cross-sections. Both lifetimes determined lifetimes are longer than those for Yb:$REVO_4$ (RE = Gd, Y and Lu) crystals, for which τ_{lum} = 247-345 μs [3].

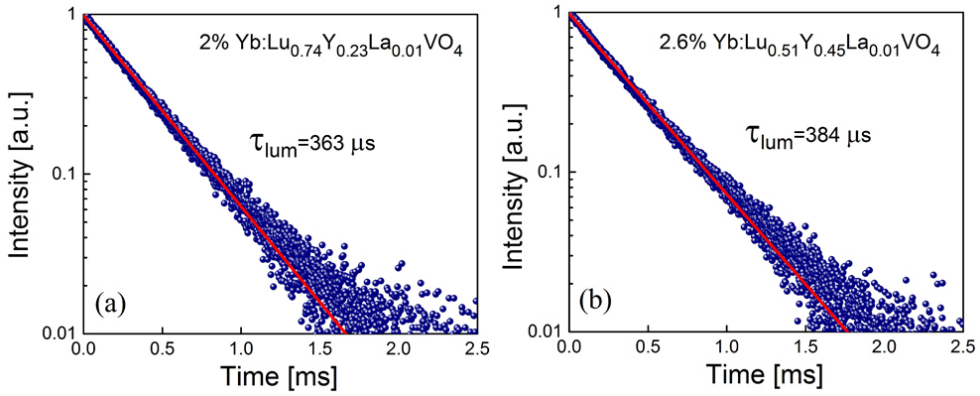

Fig. 4. Room-temperature (293 K) luminescence decay curves for powdered (a) 2 at.% Yb:$Lu_{0.74}Y_{0.23}La_{0.01}VO_4$ and (b) 2.6 at.% Yb:$Lu_{0.51}Y_{0.45}La_{0.01}VO_4$ crystals, λ_{lum} = 1010 nm, λ_{exc} = 980 nm. Symbols are the experimental data, red lines are their single-exponential fits.

The Stark splitting of the Yb^{3+} multiplets has been determined with low-temperature (LT, 6 K) absorption and emission spectroscopy for polarized light assuming J + 1/2 splitting of each multiplet, see Fig. 5.

Optical Materials EXPRESS

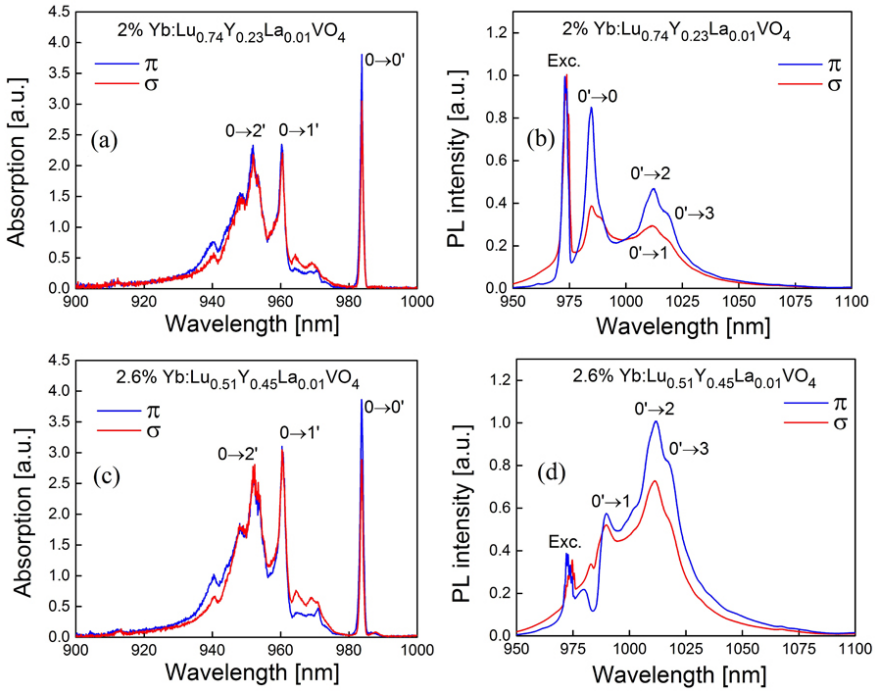

Fig. 5. Low-temperature (6 K) spectroscopy of (a,b) 2 at.% Yb:$Lu_{0.74}Y_{0.23}La_{0.01}VO_4$ and (c,d) 2.6 at.% Yb:$Lu_{0.51}Y_{0.45}La_{0.01}VO_4$ crystals: (a, c) absorption spectra and (b, d) photoluminescence (PL) spectra, λ_{exc} = 973 nm, for π and σ light polarizations.

The absorption and emission lines corresponding to the $0 \rightarrow j'$ and $0' \rightarrow i$ transitions are assigned (here, the indices i = 0-3 and j' = 0'-2' are the sub-levels of the $^2F_{7/2}$ ground-state and $^2F_{5/2}$ excited-state, respectively). This allowed us to plot the scheme of the energy levels of Yb^{3+} in the studied crystals, Fig. 6. In this figure, the calculated partition functions [18] for both multiplets $Z_{1(2)}$ are indicated, i.e., for Yb:$Lu_{0.74}Y_{0.23}La_{0.01}VO_4$, Z_1 ($^2F_{7/2}$) = 1.82 and Z_2 ($^2F_{5/2}$) = 1.48, so that Z_1/Z_2 = 1.23.

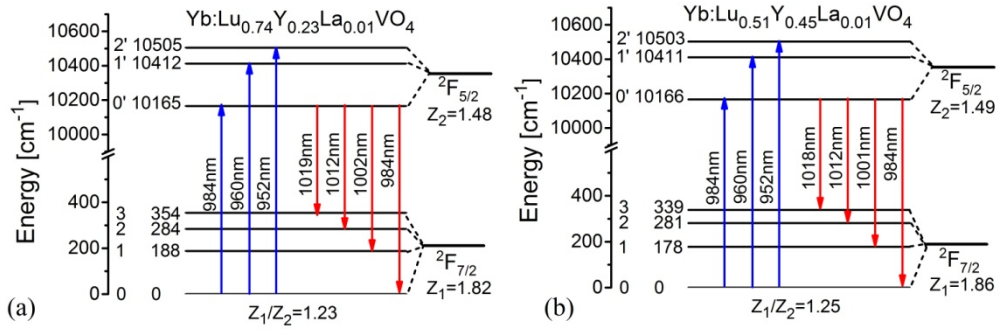

Fig. 6. Stark structure of the energy levels of Yb^{3+} in (a) $Lu_{0.74}Y_{0.23}La_{0.01}VO_4$ and (b) $Lu_{0.51}Y_{0.45}La_{0.01}VO_4$ crystals, $Z_{1(2)}$ are the partition functions, *numbers* denote the energies of the 0-3 ($^2F_{7/2}$) and 0'-2' ($^2F_{5/2}$) sub-levels (in cm^{-1}), *arrows* indicate the transitions in absorption (*blue*) and emission (*red*) at low temperature and the corresponding wavelengths

In Fig. 7, the so-called barycenter plot is presented for different Yb^{3+}-doped crystals [20] where the barycenter energy of the $^2F_{5/2}$ excited-state is plotted vs. the barycenter energy of the $^2F_{7/2}$ ground-state. For RE^{3+}, the barycenter of any $^{2S+1}L_J(4f^n)$ multiplet shows a linear variation with the barycenter of any other isolated $4f^n$ multiplet. For Yb^{3+}, this dependence is

Optical Materials EXPRESS

expressed by the formula $\langle E\rangle(^2F_{5/2}) = 10166.6 + 0.997\langle E\rangle(^2F_{7/2})$ cm^{-1} [20]. The determined Stark splitting is well in line with this trend.

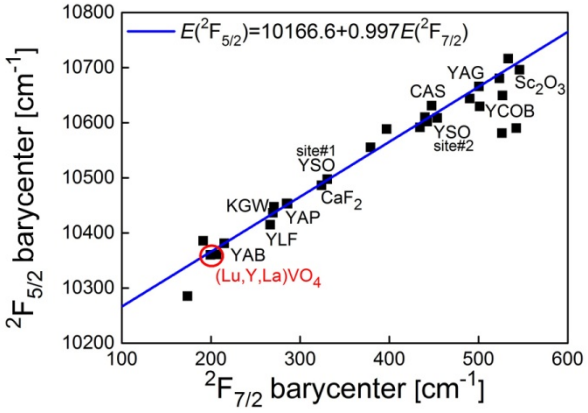

Fig. 7. A barycenter plot for Yb^{3+} in different crystals (barycenter energy $\langle E\rangle$ for the $^2F_{5/2}$ upper laser level vs. $\langle E\rangle$ for the $^2F_{7/2}$ ground-state): *symbols* – experimental data, *line* – their linear fit. Crystals: KGW – $KGd(WO_4)_2$, YLF – $LiYF_4$, YAP – $YAlO_3$, YAB – $YAl_3(BO_3)_4$, YSO – Y_2SiO_5, CAS – $Ca_2Al_2SiO_7$, YAG – $Y_3Al_5O_{12}$, YCOB –$YCa_4O(BO_3)_3$.

Based on the determined Stark splitting and using the modified reciprocity method [21], we calculated the radiative lifetimes of the $^2F_{5/2}$ state as τ_{rad} = 305 μs ($Yb:Lu_{0.74}Y_{0.23}La_{0.01}VO_4$) and 325 μs ($Yb:Lu_{0.51}Y_{0.45}La_{0.01}VO_4$). The difference in τ_{rad} and τ_{lum} (cf. Figure 4) reflects the effect of radiation-trapping on the measured luminescence decay curves. Still, the radiative lifetime for $Yb:Lu_{0.51}Y_{0.45}La_{0.01}VO_4$ is longer and both values are longer than those for the $Yb:REVO_4$ crystals [6].

According to the quasi-three-level nature of the Yb^{3+} laser, the gain cross-sections, $\sigma_{gain} = \beta\sigma_{SE} - (1-\beta)\sigma_{abs}$, were calculated, see Fig. 8. Here, $\beta = N_2(^2F_{5/2})/N_{Yb}$ is the inversion ratio. For both π and σ light polarizations, the σ_{gain} spectra are smooth and broad. The gain bandwidth (FWHM) is 41 nm (π) or 33 nm (σ) for $Yb:Lu_{0.74}Y_{0.23}La_{0.01}VO_4$ and 39 nm (π) or 29 nm (σ) for $Yb:Lu_{0.51}Y_{0.45}La_{0.01}VO_4$ (for β = 0.2) indicating high suitability of the grown crystals for broadly tunable and sub-100-fs ML lasers. Indeed, the determined gain bandwidths are broader than those calculated for $Yb:YVO_4$ and $Yb:Gd_{0.64}Y_{0.36}VO_4$ at the same inversion level for π-polarization (32 nm and 33.5 nm, respectively) [13].

Optical Materials EXPRESS

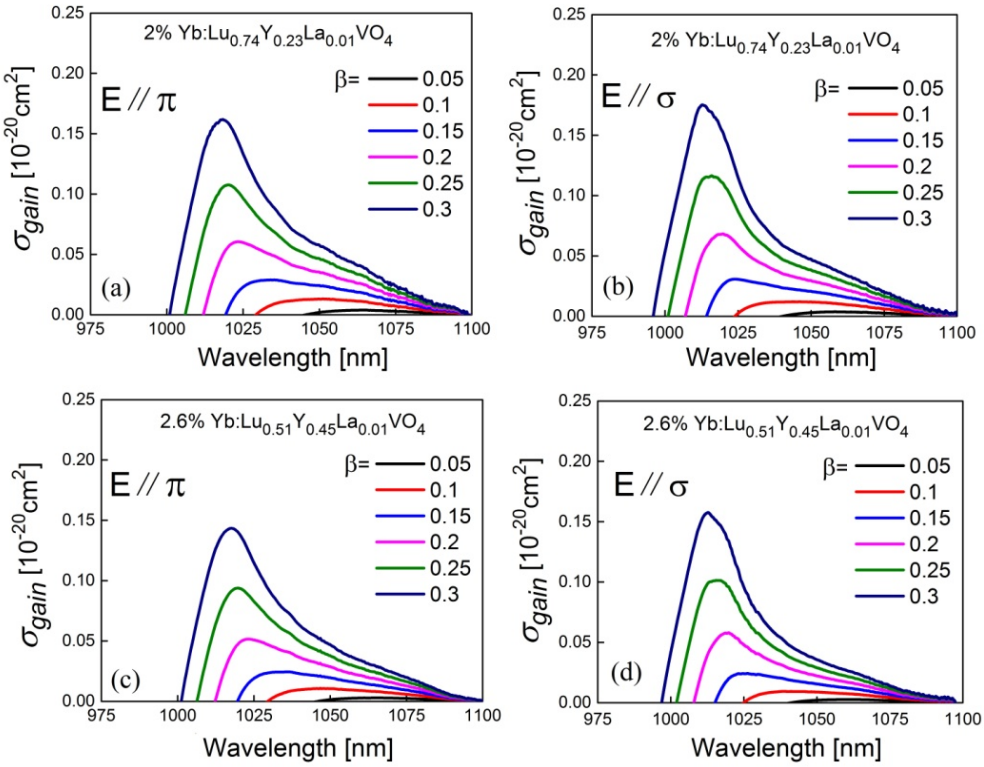

Fig. 8. (a, b) Gain cross-sections, $\sigma_{gain} = \beta\sigma_{SE} - (1-\beta)\sigma_{abs}$, for the $^2F_{5/2} \rightarrow {}^2F_{7/2}$ transition of Yb^{3+} in $Lu_{0.74}Y_{0.23}La_{0.01}VO_4$ for π (a) and σ (b) polarizations, $\beta = N_2(^2F_{5/2})/N_{Yb}$ is the inversion ratio. Figure 8. (c, d) Gain cross-sections, $\sigma_{gain} = \beta\sigma_{SE} - (1-\beta)\sigma_{abs}$, for the $^2F_{5/2} \rightarrow {}^2F_{7/2}$ transition of Yb^{3+} in $Lu_{0.51}Y_{0.45}La_{0.01}VO_4$ for π (c) and σ (d) polarizations.

4. Laser operation

For the laser experiments, the crystals were oriented for light propagation along the ***a***-axis (***a***-cut). The dimensions were 3 (***a***) × 3 (***c***) × 3 (***a***) mm^3; both input and output faces were polished to laser quality and remained uncoated. The crystals were wrapped using In foil to improve the thermal contact from all 4 lateral sides and mounted in a Cu-holder water-cooled to 12 °C. Two laser cavities were designed.

Cavity #1 (compact plane-concave) was formed by a concave (R = 100 mm) pump mirror (PM) highly reflective (HR) coated for 1.01-1.2 μm and with high transmission (HT) at the pump wavelength (~980 nm), and a flat output coupler (OC) having a transmission T_{OC} of 5% at 1.01-1.1 μm. The crystal was placed close to the PM. The total cavity length L_{cav} was ~20 mm. Cavity #2 (microchip-type) utilized a flat PM with a similar coating and a set of flat OCs with T_{OC} = 1%, 2.5%, 5% or 10%. Both PM and OC were placed close to the crystal surfaces resulting in L_{cav} ~3 mm. The crystal was pumped by fiber-coupled (fiber core diameter: 200 μm, numerical aperture, N.A. = 0.22) InGaAs laser diodes emitting unpolarized output at ~978 nm (up to 25 W and 17 W for cavity #1 and #2, respectively). A lens assembly (1:1 re-imaging ratio, f = 30 mm) was used to collimate and focus the pump radiation. The pump spot radius in the crystal w_p was 100 μm and the confocal parameter $2z_R$ was 1.8 mm.

The input-output dependences for cavity #1 are shown in Fig. 9. For both crystals, the laser output was linearly polarized (π) with the polarization naturally-selected by the anisotropy of the gain. The $Yb:Lu_{0.74}Y_{0.23}La_{0.01}VO_4$ laser generated 5.0 W at ~1044 nm with a slope efficiency η of 43% (with respect to the absorbed pump power P_{abs}). The laser threshold was at P_{abs} = 4.3 W. The output performance for the $Yb:Lu_{0.51}Y_{0.45}La_{0.01}VO_4$ laser was

Optical Materials EXPRESS

inferior: The maximum output power reached 4.15 W at lower η of 33% and higher threshold, (4.9 W). For both crystals, the input-output dependences was linear at least up to P_{abs} = 16 W.

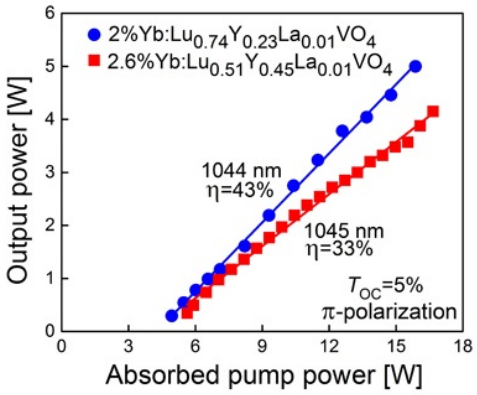

Fig. 9. Input-output dependences of cavity #1 for CW Yb:$Lu_{1-x-y}Y_xLa_yVO_4$ lasers, η – slope efficiency.

The results obtained with the microchip-type cavity and the Yb:$Lu_{0.74}Y_{0.23}La_{0.01}VO_4$ crystal are shown in Fig. 10 (a, b). Microchip laser operation with the Yb:$REVO_4$ crystals is possible due to the positive dn/dT coefficients, and, consequently, positive sign of the thermal lens [4]. The maximum output power was 2.01 W at 1033-1038 nm with η = 37% (for T_{OC} = 5%). Further power scaling was limited by the available pump power. With the increase of T_{OC}, the emission wavelength shortened from 1045 to 1050 nm (for T_{OC} = 1%) to 1023-1027 nm (for T_{OC} = 10%), in agreement with the gain spectra, see Fig. 8(a). The multi-peak emission from the microchip-type laser was related to etalon effects. The output of the microchip laser was also naturally π-polarized.

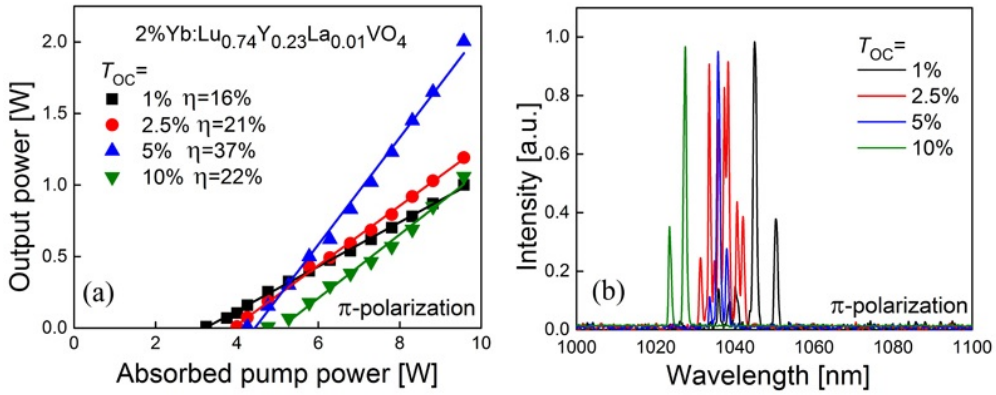

Fig. 10. Input-output dependences and typical laser emission spectra measured at maximum P_{abs} for CW Yb:$Lu_{1-x-y}Y_xLa_yVO_4$ lasers with microchip-type laser cavity #2, η – slope efficiency.

5. Conclusion

The tetragonal Yb:$Lu_{1-x-y}Y_xLa_yVO_4$ crystals offer strongly polarized spectral bands (absorption and emission) with enhanced inhomogeneous broadening compared to previously reported "mixed" orthovanadates. For Yb:$Lu_{0.74}Y_{0.23}La_{0.01}VO_4$, the FWHM of the ZPL absorption peak is >10 nm, the stimulated-emission cross-section σ_{SE} is 1.1 × 10^{-20} cm^2 at ~1013 nm and the gain bandwidth is >40 nm (for π-polarization). Moreover, this crystal features relatively long radiative lifetime of the upper laser level, ~305 μs. Multi-watt CW

Optical Materials EXPRESS

laser output at ~1044 nm is demonstrated in the Yb:$Lu_{1-x-y}Y_xLa_yVO_4$ crystals under diode-pumping at 978 nm. The new crystals are very promising for sub-100 fs ML oscillators and broadly tunable lasers around 1 μm.

Funding

National Natural Science Foundation of China (No.61575199, No.11404332, No.J1103303, No.61775039); Key Project of Science and Technology of Fujian Province (2016H0045); Strategic Priority Research Program of the Chinese Academy of Sciences (No.XDB20000000); Instrument Project of Chinese Academy of Sciences (YZ201414) and the Fund of Key Laboratory of Optoelectronic Materials Chemistry and Physics, Chinese Academy of Sciences (2008DP173016); Spanish Government (MAT2016-75716-C2-1-R, (AEI/FEDER,UE), TEC 2014-55948-R); Generalitat de Catalunya (2014SGR1358).

Acknowledgments

F. D. acknowledges additional support through the ICREA academia award 2010ICREA-02 for excellence in research. P. L. acknowledges financial support from the Government of the Russian Federation (Grant No. 074-U01) through ITMO Post-Doctoral Fellowship scheme.